Hindawi
International Journal of Electrochemistry
Volume 2019, Article ID 6759478, 12 pages
https://doi.org/10.1155/2019/6759478

Research Article

Synthesis of 1,2,3-Triazole Derivatives and Its Evaluation as Corrosion Inhibitors for Carbon Steel

Gabriel O. Resende,[1] Sara F. Teixeira,[2] Igor F. Figueiredo,[1] Alexandre A. Godoy,[2] Dafne Júlia F. Lougon,[2] Bruno A. Cotrim,[1] and Flávia C. de Souza[2]

[1]*Instituto Federal de Educação Ciência e Tecnologia do Rio de Janeiro, Campus Rio de Janeiro, 20270-021 Rio de Janeiro, RJ, Brazil*
[2]*Instituto Federal de Educação Ciência e Tecnologia do Rio de Janeiro, Campus São Gonçalo, 24425-005 São Gonçalo, RJ, Brazil*

Correspondence should be addressed to Flávia C. de Souza; flavia.souza@ifrj.edu.br

Received 1 November 2018; Accepted 8 January 2019; Published 22 January 2019

Academic Editor: Adalgisa Rodrigues de Andrade

Heterocyclic compounds containing the 1,2,3-triazole moiety can be synthesized through click-chemistry, which is rapid reactions with good yields allowing the synthesis of great derivatives diversity by making minor changes in the reagents. The products were obtained with good yields through a synthetic route which uses ready available nonexpensive commercial reagents and without any further purification of any product or intermediate. The carbon steel anticorrosive activity was tested through weight loss and electrochemical assays in acid media. It was observed relevant inhibition efficiency (> 90%) for inhibitors **1** and **2**. From Langmuir isotherm, it was hypothesized the adsorption of inhibitors on the carbon steel surface might occur by physical and chemical interaction; however, the activation energy raised suggests a physisorption process for the interaction of the inhibitor on the carbon steel surface.

1. Introduction

Heterocyclic compounds have a great diversity of physical, chemistry, and biological properties which provide them a wide range of practical uses. This chemistry class is largely used in the pharmaceutical industry both in commercial products and in research and development and more recently they are gaining attention in researches for the development of new anticorrosive compounds [1, 2].

Compounds containing 1,2,4-triazole moiety are widely studied as anticorrosive for copper [3–5] and mild steel in hydrochloric acid [6–8], phosphoric acid [9], and nitric acid [9]. Although not widely studied, the use of 1,2,3-triazole derivatives as an anticorrosive for steel [10, 11] can be found in the literature.

Compounds containing the 1,2,3-triazole moiety can be synthesized through click-chemistry, which is rapid reactions with good yields allowing the synthesis of a great derivatives diversity by making minor changes in the reagents. The copper-catalyzed 1,3-dipolar cycloaddition reaction between an azide and an alkyne is widely used for the synthesis of compounds with the 1,2,3-triazole ring with substituents in position 4 [12]. Other methodology for the synthesis of this class of compounds is the reaction of an azide with methylenic activated compounds, using different catalysts generating a triazol with substituents in positions 4 and 5 [13].

The objective of the present work is the synthesis of 1,2,3-triazole derivatives (Figure 1) and evaluation of their activity as corrosion inhibitor for carbon steel in corrosive environments.

2. Experimental

Reactions progress was monitored by TLC on aluminum sheets precoated with silica gel 60 (HF-254, Merck), film thickness of 0.25 mm. Nuclear magnetic resonance (^{1}H and ^{13}C NMR) spectra were recorded using a Varian 500 MHz instrument. For the ^{1}H NMR spectra, chemical shifts (δ) are referenced from tetramethylsilane (TMS; 0.00 ppm) and the coupling constants (J) are reported in Hz. Fourier transform infrared (FT-IR) spectra of triazole derivatives were obtained at 25°C in a Bruker Alpha spectrophotometer using the attenuated total reflectance (ATR) module.

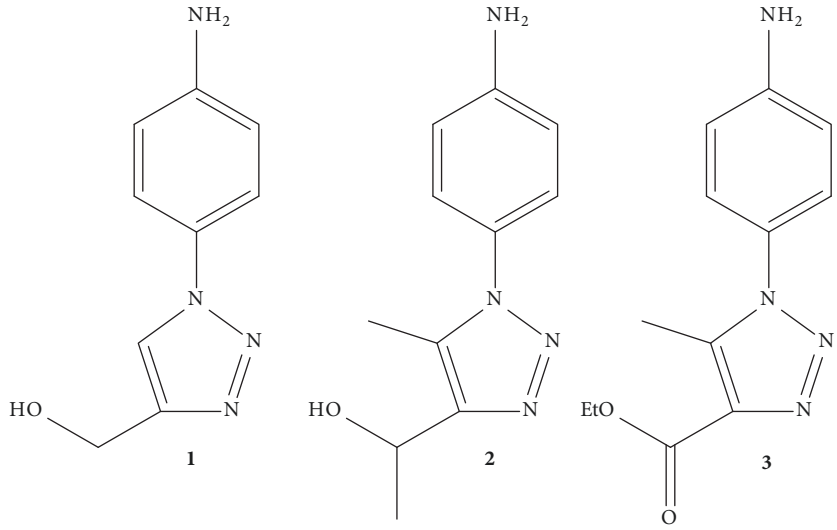

Figure 1: 1,2,3-Triazole derivatives structures.

All reagents and solvents used were commercially available and were employed without further purification unless specifically indicated.

2.1. Inhibitor Synthesis

*Synthesis of 1-azido-4-nitrobenzene (**5**).* In a flask previously containing HCl 6N (30 mL), *p*-nitroaniline (3 g, 21.74 mmol) was added with magnetic stirring at room temperature. Afterwards, a solution of $NaNO_2$ (1.5 g, 21.74 mmol) in 20 mL of water was added dropwise controlling the temperature at 5-10°C. The reaction was stirred for 1 h at room temperature and a solution of NaN_3 (1.41 g, 21.74 mmol) in 20 mL of water was added, slowly, under vigorous stirring. The reaction was followed by thin layer chromatography (TLC) and product was filtered, washed with water, and dried. The product was obtained as a yellowish solid yield: 90% (3.2 g).

FT ATR IR 3069 (C-H ar st), 2120 (N_3 st), 1590 (ar C=C st), 1512 (C-NO_2 ass st), 1287 (C-NO_2 sym st).

*Synthesis of (1-(4-nitrophenyl)-1H-1,2,3-triazol-4-yl)methanol (**7**).* To a suspension of (**5**) (1.2 g, 7.32 mmol) in *terc*-butanol (5 mL) was added a mixture of ascorbic acid (281 mg, 1.6 mmol), $CuSO_4.5H_2O$ (145 mg, 0.58 mmol), and $NaHCO_3$ (135 mg, 1.6 mmol) in 5.5 mL of water. Afterwards, propargylic alcohol (0.52 mL, 9 mmol) was added and the reaction mixture was stirred for 24-48 h at room temperature. The reaction was followed by TLC and the product was obtained by filtration, washed with water, and dried. The product was obtained as a brownish solid and was used without further purification in next step, yield 78% (1.25 g).

FT-IR (ATR) 3436 (O-H st), 1598 (ar C=C st), 1510 (C-NO_2 ass st), 1287 (C-NO_2 sym st).

*Synthesis of (1-(4-aminophenyl)-1H-1,2,3-triazol-4-yl)methanol (**1**).* To a suspension of (**7**) (1.54 g, 7.0 mmol) in water (40 mL), NH_4Cl (750 mg, 14 mmol) and zinc powder (3.325 g, 50.8 mmol) were added. The reaction mixture was stirred and heated to 80°C during 3 hours. The resulting mixture was filtered and washed with dichloromethane. The aqueous phase was extracted with dichloromethane five times. The organic phase was dried over Na_2SO_4, filtered, and concentrated to obtain the product as a pinkish solid, yield of 68% (0.90 g).

FT-IR (ATR) 3462 (O-H st), 3362 (N-H st), 1631 (ar C=C st), 860 (ar C-H δ).

^{1}H NMR (500 MHz, DMSO-d_6) δ 8.28 (s, 1H), 7.45-7.43 (d, J=9.0 Hz, 2H), 6.71-6.69 (d, J=8.5 Hz, 2H), 5.32 (s, 2H), 5.05 (s, 1H), 4.58 (s, 2H).

^{13}C NMR (22.5 MHz, DMSO-d_6) δ 149.22, 148.48, 126.26, 121.54, 120.62, 113.93, 55.06.

*Synthesis of ethyl 1-(4-nitrophenyl)-5-methyl-1H-1,2,3-triazole-4-carboxylate (**6**).* To a round bottom flask of 50 mL were added 276 mg (2 mmol) of compound **5** and 1 mL of DMF and the solid was solubilized with magnetic stirrer at room temperature. Afterwards, 0.6 mL of trimethylamine and 0.55 mL of ethyl acetoacetate were added to the flask. The reaction mixture was stirred at room temperature for 24 hours. The reaction was followed by thin layer chromatography. The work up of the product was made through filtration. The reaction had a yield of 94% (436 mg), brownish solid.

FT ATR IR 3080 (C-H ar st), 2976 (C-H aliph st), 1711 (C=O st), 1530 (C-NO_2 assym st), 1343 (C-NO_2 sym st), 852 (ar C-H δ).

*Synthesis of ethyl 1-(4-aminophenyl)-5-methyl-1H-1,2,3-triazole-4-carboxylate (**3**).* In a round bottom flask of 100 mL were added 332 mg (1,3 mmol) of compound **6,** 50 mg of palladium 10% supported on active charcoal 10%, 375 mg of ammonium formate, and 2 mL of methanol. The reaction was maintained under nitrogen atmosphere with magnetic stirring and room temperature for 24 hours. The reaction was followed by thin layer chromatography. The reaction mixture was filtered through Celite and the Celite was washed with 10 mL of dichloromethane. The filtrate was extracted with brine; the organic phase was dried with Na_2SO_4 anhydrous

and then distilled under reduced pressure. The product was obtained as a white solid with a yield of 83.2% (244 mg).

FT-IR (ATR) 3345 (N-H st), 2978 (C-H st), 1702 (C=O st), 1516 (ar C=C st)), 840 (ar C-H δ).

^{1}H NMR (500 MHz, DMSO-d_6) δ 7.17-7.16 (d, J=9.0 Hz, 2H), 6.73-7.72 (d, J=9.0 Hz, 2H), 5.50 (S, 1H), 4.37-4.32 (q, J=7.5 Hz, 2H), 2.43 (s, 3H), 1.35-1.32 (t, J=7.5, 3H).

^{13}C NMR (125 MHz, DMSO-d_6) δ 161.70, 150.71, 139.36, 135.93, 126.75, 123.90, 114.23, 60.67, 14.60, 10.04.

*Synthesis of 1-(5-methyl-1-(4-nitrophenyl)-1H-1,2,3-triazol-4-yl)ethanone (**8**).* To a round bottom flask of 10 mL were added 693 mg (3.2 mmol) of compound **5** and 1.7 mL of DMF and the solid was solubilized with magnetic stirrer at room temperature. Afterwards, 1.2 mL of trimethylamine and 0.9 mL of ethyl acetylacetone were added to the flask. The reaction mixture was stirred at room temperature for 24 hours. The reaction was followed by thin layer chromatography. The work up of the product was made through filtration. The product was obtained as a solid powder with a 75.5% yield (740 mg).

FT ATR IR 3076 (C-H ar st), 1677 (C=O st), 1518 (C-NO_2 assym st), 1341(C-NO_2 sym st), 853 (ar C-H δ)

*Synthesis of 1-(1-(4-aminophenyl)-5-methyl-1H-1,2,3-triazol-4-yl)ethanol (**2**).* In a 10 mL round bottom flask was added compound 208 mg of compound **8**, 5 mL of methanol, and 0.8 mL of an aqueous saturated solution of $CuSO_4$. In a second flask it was prepared a solution of 190 mg of $NaBH_4$ in 6 mL of a mixture of water/methanol 1:1. Under ice bath (5-10°C) the content of the second flask was added dropwise to the first flask and it was observed the formation of a CuS black precipitate. The reaction was followed by thin layer chromatography. The CuS precipitated was filtered and methanol was distilled under reduced pressure. The concentrate was solubilized in ethyl acetate and extracted with water. The organic phase was dried with anhydrous Na_2SO_4 and the solvent was distilled under reduced pressure. The product was obtained as a purplish solid with 79% yield (144 mg)

FT-IR (ATR) 3466 (O-H st), 3326 (N-H st), 2972 (C-H st), 1517 (ar C=C st), 837 (ar C-H δ).

^{1}H NMR (500 MHz, DMSO-d_6) δ 7.10-7.09 (d, J=8.5 Hz, 2H), 6.71-6.70 (d, J=8.5 Hz, 2H), 5.38 (s, 2H), 4.92-4.88 (m, 2H), 2.23 (s, 3H), 1.50-1.49 (d, J=6.5, 3H).

^{13}C NMR (125 MHz, DMSO-d_6) δ 150.09, 147.89, 130.49, 126.40, 114.25, 62.12, 23.52, 9.02.

2.2. Gravimetric Weight Loss. Carbon steel used as specimens was cut into 3.0 cm × 1.0 cm × 1.0 cm sections and abraded with emery paper of different granulometry (320, 600, and 1000). The chemical composition ASTM 1020 carbon steel is (wt%): C (0.18%), Mn (0.30%), S (0.05%), and Fe (balance). These pieces were washed with double distilled water, degreased with acetone, and dried in air.

Triplicate specimens were immersed in a 1.0 mol L^{-1} HCl aqueous solution prepared from 37% HCl (purchased from Merck Co. Darmstadt, Germany) and double distilled water, in the absence and presence of corrosion inhibitors at 250 mg L^{-1}, for a period of 24 h. After the specimens were removed, washed with water and acetone, and dried in warm air, the weight was obtained according to ASTM G31-72 [ASTM International G31-72: Standard practice for laboratory Immersion Corrosion Testing of Metals. West Conshohocken: ASTM International; 1999] (standard method) and determined using an analytical balance with a 0.1 mg precision. The efficiency of inhibition ($E.I.$%) was calculated using

$$E.I.(\%) = \frac{W_0 - W}{W_0} \times 100 \quad (1)$$

where W_0 and W are the weight loss (g cm^{-2} h^{-1}) in the absence (blank) and presence of the corrosion inhibitor compound, respectively. The corrosion rate in millimeters penetration per year (mm/y) was obtained

$$W = \frac{K\,M}{A\,t\,\rho} \quad (2)$$

where K is a constant (8.76×10^4), M is the weight loss in grams, A is the specimen area in cm^2, t is time in hour, and ρ is the specific mass of carbon steel (7.86 g cm^{-3}).

The gravimetric testing was also performed at different inhibitor concentrations (250–1250 mg L^{-1}), different immersion times (4, 8, 12, 24, and 48 h), and different temperatures (25, 35, 45, and 55°C).

2.3. Electrochemical Experiments. Electrochemical measurements were carried out in conventional three-electrode cell (100 mL) using a Microautolab III/FRA2 (Eco Chemie; Utrecht, the Netherlands) coupled to a personal computer and controlled with GPES 4.9 software (General Purpose Electrochemical System). In all cases, ASTM was used as standard method. The supporting electrolyte was the same used in loss weight and the measurements were carried out in 100 mL of nonstirred and naturally aerated electrolyte maintained at 25°C.

Carbon steel specimens with same composition used in the gravimetric weight loss measurements were cut and employed as work electrode with exposed surface area of 0.78 cm^2. These carbon steel electrodes also were abraded in politriz Aropol 2V (Arotec) with emery paper of different granulometry (320, 400, 600, and 1000), washed with double distilled water, degreased with acetone, and dried in air. Saturated calomel electrode (SCE) was used as the reference electrode, and a Pt wire with large superficial area was used as the auxiliary electrode.

Work electrode in electrochemical measurements was kept in support electrolyte during 1 h to reach its stable open-circuit potential (OCP). Electrochemical impedance spectroscopy (EIS) was performed using the aforementioned potentiostat over a frequency range of 100 kHz to 10 mHz at the stable open-circuit potential with an AC wave of 10 mV (rms). Potentiodynamic polarization curves were also obtained after 1 h in the open-circuit potential and performed using a scan rate equal to 1 mV s^{-1} from –300 mV up to +300 mV in relation to OCP.

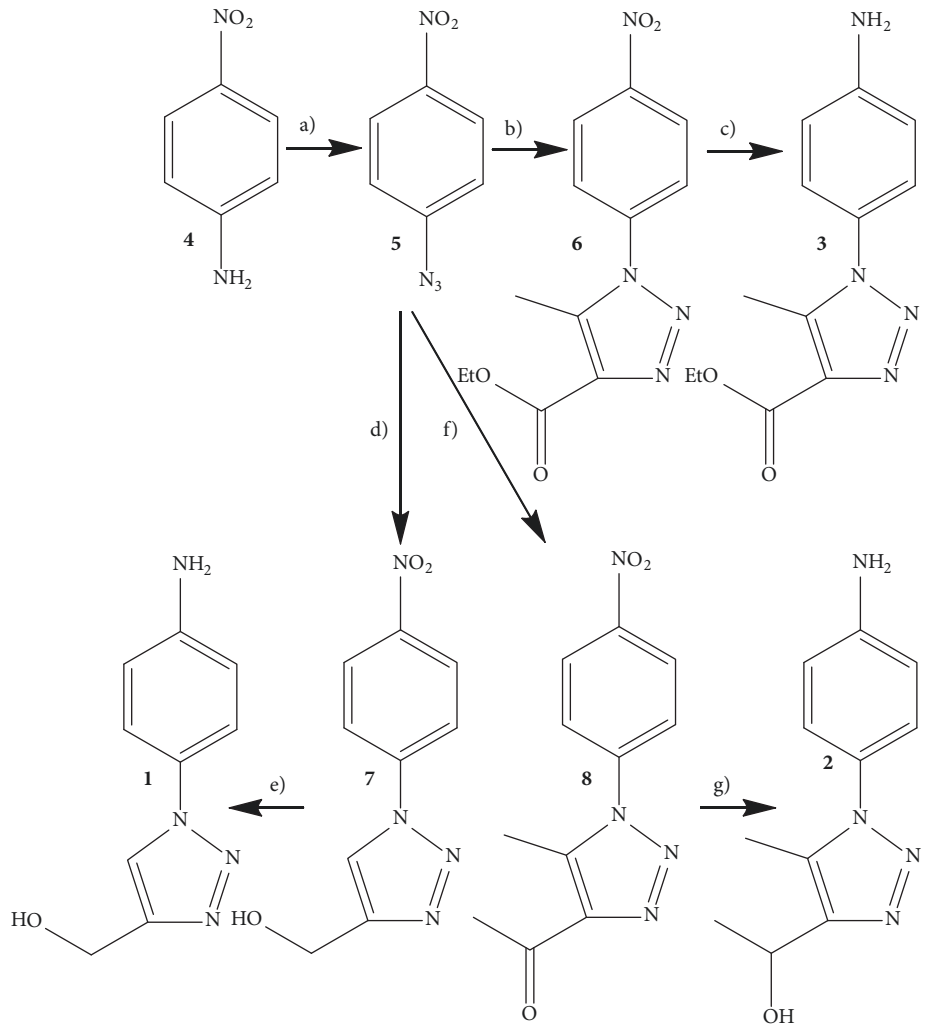

Scheme 1: Synthetic route to triazole derivatives compounds **3–8**: (a) (1) $HCl/NaNO_3$ (2) NaN_3; (b) Ethyl Acetoacetate, Et_3N, DMF; (c) Pd/C, ammonium formate; (d) (1) Ascorbic Acid, $CuSO_4.5H_2O$, $NaHCO_3$ (2) Propargylic Alcohol; (e) Zn, NH_4Cl/H_2O; (f) Et_3N, Acetylacetone; (g) $NaBH_4$/MeOH, $Cu_2SO_4.5H_2O$.

The synthetic inhibitors with the best inhibitory efficiency (*I.E.*%) by gravimetric weight loss were subjected to the electrochemical testing of OCP, EIS measurements, and polarization curves. The *I.E.*(%) value was also obtained from potentiodynamic polarization curves and EIS diagrams from

$$I.E.\,(\%) = \frac{j_{corr,0} - j_{corr}}{j_{corr,0}} \times 100 \quad (3)$$

where $j_{corr,0}$ and j_{corr} are the corrosion current density obtained from Tafel plots in the absence and presence of an inhibitor. The *I.E.*(%) value from EIS diagrams was calculated from

$$I.E.\,(\%) = \frac{R_{ct} - R_{ct,0}}{R_{ct}} \times 100 \quad (4)$$

were $R_{ct,0}$ and R_{ct} are the charge transfer resistance in the presence and absence of the inhibitor, both obtained from the EIS diagrams by extrapolation of the semicircle.

3. Results and Discussions

3.1. Inhibitor Synthesis and Characterization. Synthetic route proposed to obtain triazoles compounds was presented in Scheme 1. Briefly, the reaction of *p*-nitroaniline (**4**) with sodium nitrite in acidic medium and addition of sodium azide was used to obtain compound **5** [12]. The intermediate **5** was reacted with ethyl acetoacetate in the presence of triethylamine to obtain compound **7** [13]. Compound **8** was obtained from reaction of intermediate **6** with propargyl alcohol catalyzed by Cu^+ [12] and compound **9** from reaction of intermediate **6** with acetoacetone in the presence of triethylamine [13]. Compounds **3** and **1** were obtained from respective reaction of **6**, **7**, and **8** with zinc in presence of ammonium chloride and water or Pd/C with ammonium formate [14]. Compound **2** was obtained from reaction of compound **8** with sodium borohydride in the presence of copper sulphate [15].

Table 1: Inhibitor efficiencies to carbon steel in 1.0 mol L^{-1} HCl solution containing 250 mg L^{-1} of commercial and proposed inhibitors after immersion for 24 h at 25°C.

Inhibitor	*I.E.* (%)	Error (%)
1	91.9	1.3
2	95.8	0.7
3	70.2	1.3
Commercial	72.2	1.9

Table 2: Inhibitor efficiencies and corrosion rates to carbon steel in 1.0 mol L^{-1} HCl solution with different concentrations of inhibitors, after immersion for 24 h at 25°C.

Inhibitor Concentration (mg L^{-1})	Inhibitor 1			Inhibitor 2			*Commercial Inhibitor*		
	W (mm/y)	*I.E.* (%)	Error (%)	*W* (mm/y)	*I.E.* (%)	Error (%)	*W* (mm/y)	*I.E.* (%)	Error (%)
Blank	12.8	–	–	12.8	–	–	12.8	–	–
250	1.0	91.9	1.3	0.5	95.8	0.7	2.2	72.2	1.9
500	0.9	93.4	0.3	0.4	96.7	0.3	1.3	82.9	1.2
750	0.7	94.3	0.8	0.6	95.5	5.5	1.3	83.1	0.9
1000	0.6	95.0	0.5	0.2	98.2	0.3	1.3	83.9	0.7
1250	0.5	96.2	0.2	0.1	99.2	0.2	0.8	84.1	0.5

The products were obtained using synthetic route using ready available nonexpensive commercial reagents and without any further purification of any product or intermediate. Products were obtained in good purity as observed in infrared and RMN analysis and yields of all synthetic steps were good varying between 60 and 94%.

3.2. Gravimetric Weight Loss Measurements. In an electrochemical spontaneous corrosion process, when the metal interacts with electrolyte solution, both anodic and cathodic reactions occur. Corrosion mechanism of carbon steel in acid solution can happen by reaction between metallic iron and H^+ producing ferrous ion (Fe^{2+}) and hydrogen gas, shown as follows [16]:

$$\mathrm{Fe + H \longrightarrow [FeH_{ads}]^+}$$
$$\mathrm{[FeH_{ads}]^+ + e^- \longrightarrow [FeH_{ads}]}$$
$$\mathrm{[FeH_{ads}] + H^+ + e^- \longrightarrow Fe + H_2}$$
$$\mathrm{Fe \longrightarrow Fe^{2+} + 2e^-}$$

The inhibition efficiency obtained from weight loss experiments with carbon steel in acid medium is presented in Table 1. An imidazoline based commercial corrosion inhibitor was used in same concentration to compare the inhibition efficiency of proposed inhibitors.

The data from Table 1 suggest that the triazole compounds behave as corrosion inhibitors and that their inhibition efficiency remains high through long periods of immersion (24 h) for low inhibitor concentration. Inhibitors **1** and **2** showed the best inhibitions efficiencies (greater than 90%) with a relative standard deviation lower than 2%. Analyzing this result, we can hypothesize that the hydroxyl group present in both compounds **1** and **2** and absent in compound **3** could be an important group with anticorrosive activity. Additional studies, as molecular docking between the synthesized inhibitors and the metal alloy, should be done in order to understand the structure–activity relationships for the synthesized triazole corrosion inhibitors. Therefore, we chose inhibitors **1** and **2** to carry out further corrosion assays and try to explain the corrosion inhibition mechanism.

The rates of carbon steel corrosion in 1.0 mol L^{-1} HCl aqueous solution, in the presence and absence of the best inhibitors, in concentration range of 250–1250 mg L^{-1} for 24 h immersion at 25°C, as well as the efficiency results, are shown in Table 2.

The carbon steel corrosion rate (*W*) shown in Table 2 was significantly reduced with addition of the inhibitors. Those results show the inhibitory effect of the triazole compounds against carbon steel corrosion in low pH solutions. Furthermore, the inhibition efficiency grew when the concentration of triazole compounds in this medium increased. It has also been observed that the inhibition efficiencies of compound **2** are higher when compared to those of compound **1**.

The corrosion process was also investigated in different immersion time of carbon steel in 1.0 mol L^{-1} HCl aqueous solution in presence and absence of 500 mg L^{-1} of inhibitors (4, 8, 12, 24, and 48 h) at room temperature and the results of the weight loss measurements are shown in Table 3.

It can be observed in Table 3 that in solutions without inhibitor the uniform corrosion rate is very severe for all immersion times (varying of 16.0 mm/y to 12.8 mm/y) and the rate was greatly reduced with the addition of the inhibitors for all immersion times, reaching 0.9 mm/y and 0.4 mm/y in the presence of the inhibitors with 24 h of immersion. These corrosion rates are considered low, according to Gentil (for cheap materials, like carbon steel, the corrosion rate could be acceptable in the range of 0.225 to 1.5 mm/y) [17].

Table 3: Inhibitor efficiencies and corrosion rates to carbon steel in 1.0 mol L^{-1} HCl aqueous solution in presence and absence of the inhibitor (500 mg L^{-1}) with different immersion times, at 25°C.

Immersion Time (h)	Blank	Inhibitor 1			Inhibitor 2		
	W (mm/y)	W (mm/y)	I.E. (%)	Error (%)	W (mm/y)	I.E. (%)	Error (%)
4	16.0	1.7	89.2	1.5	0.3	97.9	0.6
8	14.7	1.8	87.5	1.9	0.3	97.9	0.2
12	14.7	1.6	88.8	0.7	0.2	98.7	0.5
24	12.8	0.9	93.4	0.3	0.4	96.7	0.3
48	14.2	1.6	88.6	1.2	0.3	97.9	0.2

Table 4: Values of the α and r of the Langmuir isotherm, K, and ΔG^0_{ads} obtained for the corrosion inhibitors.

Inhibitor	Parameters of Langmuir isotherm			
	α	r	K (L $mmol^{-1}$)	ΔG^0_{ads} (KJ mol^{-1})
1	1.027	0.9999	9.25	−33.6
2	0.998	0.9991	11.36	−33.1

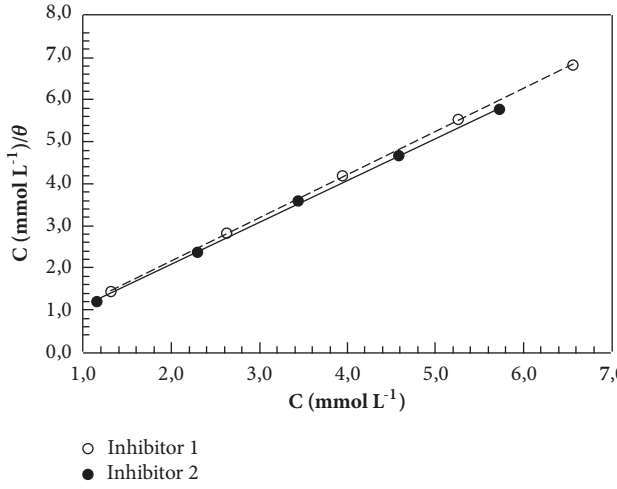

Figure 2: Langmuir adsorption isotherms of triazole compounds on the carbon steel surface in 1.0 mol L^{-1} HCl aqueous solution.

Corrosion rate reduction in presence of inhibitors occurs due to the formation of protective layer by inhibitor adsorption on the metallic surface. To investigate the adsorption behavior of triazole compounds, various isotherms were used and Langmuir isotherm was the best fit with the experimental data from Table 2. Langmuir isotherm was obtained from linear correlation between the level of surface coating (θ) and inhibitor concentration (C). The adsorption isotherm used is plotted assuming that all adsorption sites are equivalent and that binding of particles is unaffected by any nearby occupied or unoccupied locations. In accordance with this isotherm, θ/C is related to C by

$$\frac{C}{\theta} = C + \frac{1}{K} \tag{5}$$

where K is the adsorption equilibrium constant. Figure 2 shows the relationship between C/θ and the concentration of inhibitors.

A linear correlation can be observed in Figure 2 with significant correlation coefficients (r), showing the validity of the isotherm (Table 4). The curve slope is near the unity, which can suggest that the inhibitor adsorbed molecules form a monolayer on carbon steel surface. The adsorption constant (K) was calculated from the Langmuir intercept and related to the standard Gibbs free energy (ΔG^0_{ads}) according to

$$K = \frac{1}{55.55} \exp\left(\frac{-\Delta G^0_{ads}}{RT}\right) \tag{6}$$

where R is the universal gas constant, T is the absolute temperature, and 55.55 mol L^{-1} is the water molar concentration in solution. Table 4 shows the values of the slope (α), the correlation coefficient (r) of the Langmuir isotherm, the adsorption constant (K), and the standard Gibbs free energy (ΔG^0_{ads}).

The ΔG^0_{ads} values obtained from (6) were −33.6 and 33.1 kJ mol^{-1} to compounds **1** and **2**, respectively. Generally, values of

Table 5: Inhibitor efficiencies and corrosion rates to carbon steel in 1.0 mol L^{-1} HCl aqueous solution in absence and presence of 250 mg L^{-1} of inhibitors during 4 h, varying temperatures.

Temperature (°C)	Inhibitor	*W* (mm/y)	*I.E.* (%)	Error (%)
25	Blank	16.0	–	–
	1	1.7	89.2	1.5
	2	0.3	97.9	0.6
35	Blank	33.6	–	–
	1	3.6	89.4	0.6
	2	0.8	97.6	1.6
45	Blank	66.1	–	–
	1	5.9	91.1	0.4
	2	2.3	96.5	0.2
55	Blank	99.8	–	–
	1	13.0	87.0	0.3
	2	5.4	94.6	0.3

ΔG^0_{ads} greater than −20 kJ mol^{-1} indicate electrostatic interactions attributed to inhibition interaction between the charged compounds and the charged metal surface (physisorption) and values equal or smaller than −40 kJ mol^{-1} are related to electrons share or electrons transfer from organic molecules of the inhibitor to the metal surface, forming a coordinate bond (chemisorption). In accordance with the ΔG^0_{ads} values obtained, it can be hypothesized that the adsorption of both compounds is not only by physisorption or chemisorption but by obeying a comprehensive adsorption (chemisorption and physisorption). It is difficult to differentiate between chemisorption and physisorption based only on these criteria, particularly when charged species are adsorbed.

The effects of temperature on the corrosion of carbon steel in 1.0 mol L^{-1} HCl solution in absence and presence of 250 mg L^{-1} of inhibitors were studied during 4 h, varying temperatures (25, 35, 45, and 55°C). The corrosion rates and inhibitor efficiencies obtained in this study were presented in Table 5.

Table 5 shows that in solutions without inhibitor the corrosion process is accentuated and increased with the temperature (varying of 16.0 mm/y to 99.8 mm/y). It can be observed that corrosion rate reduces with the addition of the inhibitors for all temperatures, in the presence of the inhibitors, and inhibition efficiencies increase. These inhibition efficiencies stay high even at high temperatures (87.0%±0.3% and 94.6%±0.3% at 55°C).

The apparent activation energy for carbon steel corrosion in absence and presence of 250 mg L^{-1} of inhibitors was determined from an Arrhenius-type plot according to

$$\ln W_{corr} = \frac{-E_a}{RT} + \ln A \tag{7}$$

where W_{corr} is corrosion rate, E_a is activation energy, A is the frequency factor, T is the absolute temperature, and R is the molar gas constant. Arrhenius plots of $\ln W_{corr}$ versus $1/T$ in the absence and presence of 250 mg L^{-1} of inhibitors are shown in Figure 3.

The apparent activation energy obtained for the corrosion process in the acid solution was 49.7 kJ mol^{-1} and in the acid solution in presence of **1** and **2** inhibitors were 55.2 and 78.8 kJ mol^{-1}, respectively (Table 6). It was clear that apparent activation energy increase with the presence of inhibitors compounds indicates the physical adsorption mechanism [18].

The corrosion inhibition process also can be explained by using thermodynamic model. The adsorption heat (ΔH^0) and the adsorption free entropy (ΔS^0) were calculated by plot of $\ln(W_{corr}/T)$ versus $1/T$ according to

$$\ln \frac{W_{corr}}{T} = \frac{\ln R}{Nh} + \frac{\Delta S^0}{R} - \frac{\Delta H^0}{RT} \tag{8}$$

where h is the Planck's constant, N is the Avogadro's number, T is the absolute temperature, and R is the universal gas constant. Straight lines of $\ln(W_{corr}/T)$ versus $1/T$ are plotted in Figure 4 and ΔH and ΔS values from the slope of $(-\Delta H^0/R)$ and an intercept of $[(\ln(R/Nh) + (\Delta S^0/2.303RT)]$, respectively, were calculated and also listed in Table 6.

The positive values of $\Delta \boldsymbol{H}$ observed in Table 6 reflect the endothermic nature of the carbon steel dissolution process which is attributed to the slower dissolution of mild steel in the presence of the inhibitor than in its absence. The negative values of $\boldsymbol{\Delta S}$ observed for uninhibited and inhibited solution due the activated complex in the rate determining step represent an association rather than dissociation, resulting in a decrease in the randomness on going from the reactants to the activated complex [19]. It was clear from Table 6 data that $\boldsymbol{Ea}$ and $\Delta \boldsymbol{H}$ values vary in the same way. The $\Delta \boldsymbol{H}$ values were lower than $\boldsymbol{Ea}$ values and it can indicate the corrosion process must involve a gaseous reaction, probably, a hydrogen evolution reaction associated with decrease in total reaction volume. These results fit the known thermodynamic relation between $\boldsymbol{Ea}$ and $\Delta \boldsymbol{H}$ described in

$$\boldsymbol{Ea} - \Delta \boldsymbol{H} = \boldsymbol{RT} \tag{9}$$

It was found that, for the whole system, the difference is 2.60 kJ mol^{-1} in HCl medium. This is the approximate value

Table 6: Thermodynamic parameters of corrosion inhibition process of carbon steel in 1.0 mol L^{-1} HCl solution in absence and presence of inhibitors.

Inhibitor	E_a (kJ mol^{-1})	r^2	ΔH (kJ mol^{-1})	ΔS (J mol^{-1} K^{-1})	r^2	$E_a - \Delta H$ (kJ mol^{-1})
blank	50.39	0.9910	47.79	–126.9	0.9918	2.597
1	52.84	0.9916	50.22	–137.7	0.9840	2.597
2	76.51	0.9998	73.91	–72.23	0.9971	2.602

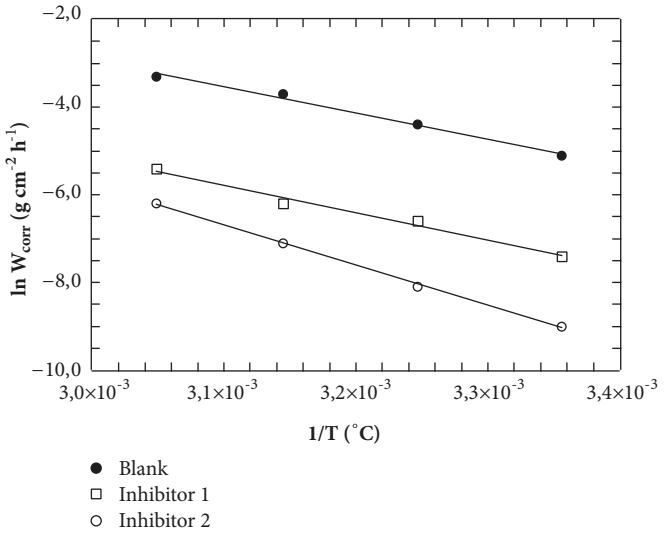

Figure 3: Arrhenius plots of ln W_{corr} versus 1/T in the absence and presence of 250 mg L^{-1} of inhibitors compounds.

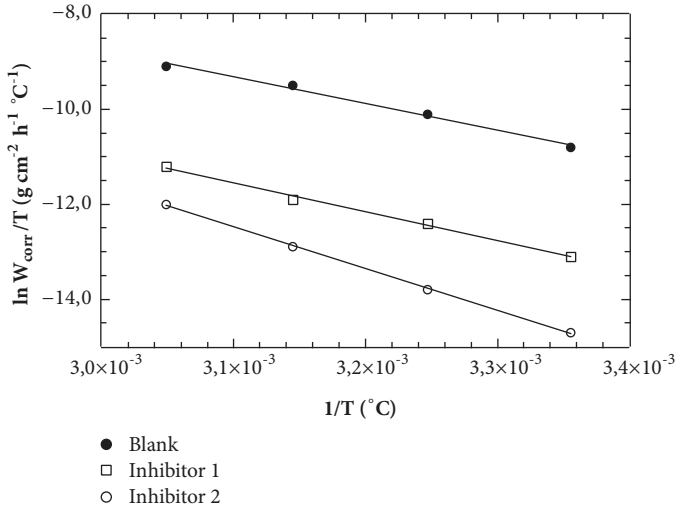

Figure 4: Adsorption heat (ΔH^0) and adsorption free entropy (ΔS^0) of triazole compounds on the carbon steel surface in 1.0 mol L^{-1} HCl aqueous solution.

estimated for RT, where T is the range of experimental temperatures.

3.3. Electrochemical Experiments

3.3.1. Potentiodynamic Polarization Curves. Figure 5 shows the potentiodynamic polarization curves of carbon steel in 1.0 mol L^{-1} HCl solution in absence and presence of different concentration of inhibitors at room temperature.

The potentiodynamic polarization curves show the inhibitors presence caused a significant decrease in cathodic and anodic current densities. These results could be explained by the adsorption of inhibitors at the active sites of the electrode surface, which also retards the metallic dissolution

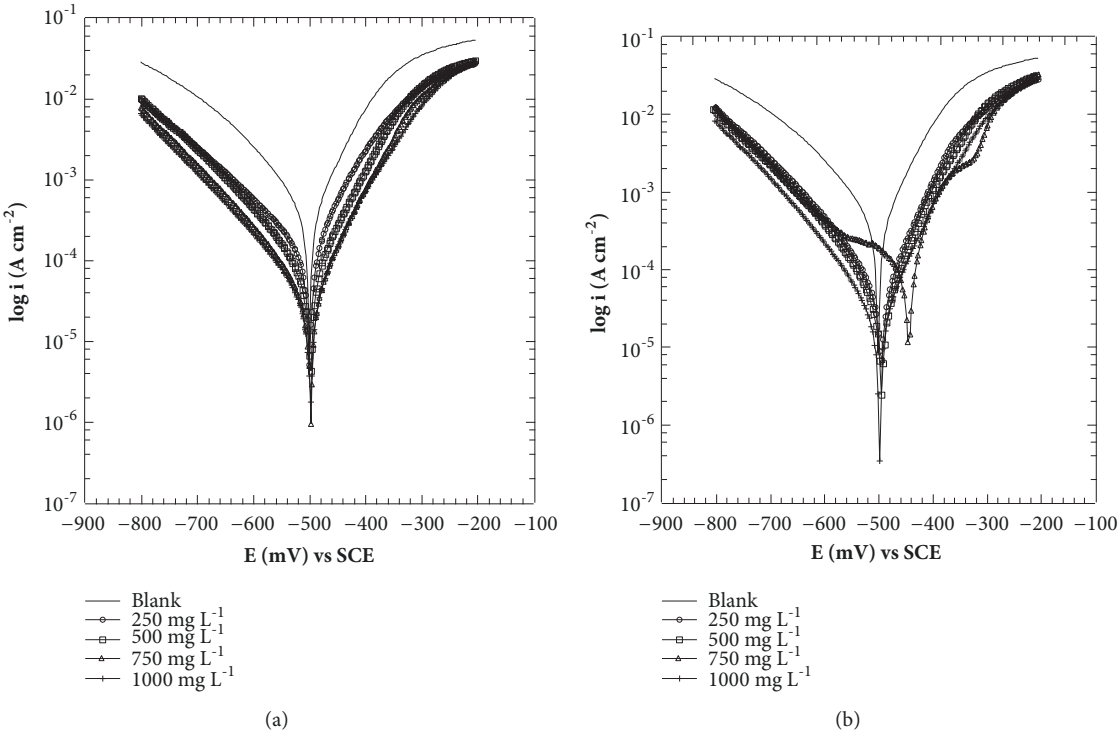

Figure 5: Potentiodynamic polarization curves of carbon steel in 1.0 mol L^{-1} HCl solution in absence and presence of different concentrations if inhibitor 1 (a) and inhibitor **2** (b).

Table 7: Electrochemical parameters of carbon steel in 1.0 mol L^{-1} HCl aqueous in absence and presence of inhibitors at different concentrations.

Inhibitor	Inhibitor Concentration (mg L^{-1})	E_{corr} (mV)	j_{corr} (mA/cm^2)	b_c (mV/dec)	b_a (mV/dec)	*I.E.* (%)
	Blank	−496.4	0.6055	180.18	101.74	
1	250	−497.6	0.2448	522.42	105.08	60
	500	−507.5	0.1157	369.12	98.09	81
	750	−496.2	0.0397	134.92	78.77	93
	1000	−492.0	0.0295	105.54	62.52	95
2	250	−494.7	0.1305	390.55	128.79	78
	500	−493.7	0.0414	132.63	79.09	93
	750	−444.1	0.0955	152.75	45.30	84
	1000	−495.9	0.0331	167.75	83.58	95

and hydrogen evolution and consequently slows the corrosion process. The electrochemical parameters, i.e., the corrosion potential (E_{corr}), corrosion current density (j_{corr}), and the anodic (b_a) and cathodic (b_c) Tafel constants, shown in Table 7, were obtained from the Tafel plots from Figure 5.

The corrosion current density (j_{corr}) decreases in the presence of both inhibitors (Table 7). There was no remarkable shift in the corrosion potential (E_{corr}) value with respect to the blank. According to literature report [20], when corrosion potential is more than ±85 mV with respect to the corrosion potential of the blank, the inhibitor can be considered distinctively as either cathodic or anodic type. However, the maximum displacement in this study is less than ±85 mV. The cathodic (b_c) and anodic (b_a) Tafel slopes are significantly changed indicating that the inhibition mechanism occurred with the addition of the inhibitors (Table 7), blocking the available cathodic and anodic active sites on the metal surface. The change in cathodic Tafel slopes is larger than that in anodic Tafel slopes, which reveals that inhibitor molecules are adsorbed on both sites but under prominent cathodic control, resulting in the inhibition of anodic dissolution and cathodic reduction. The inhibition efficiency calculated from the j_{corr} values obtained in the absence and presence of inhibitors varied from 60 to 95% in inhibitor **1** and 78 to 95% in inhibitor **2**, over a concentration range of 250–1000 mg L^{-1}. These results of the inhibition efficiencies revealed a fairly good inhibition action of synthetic inhibitors.

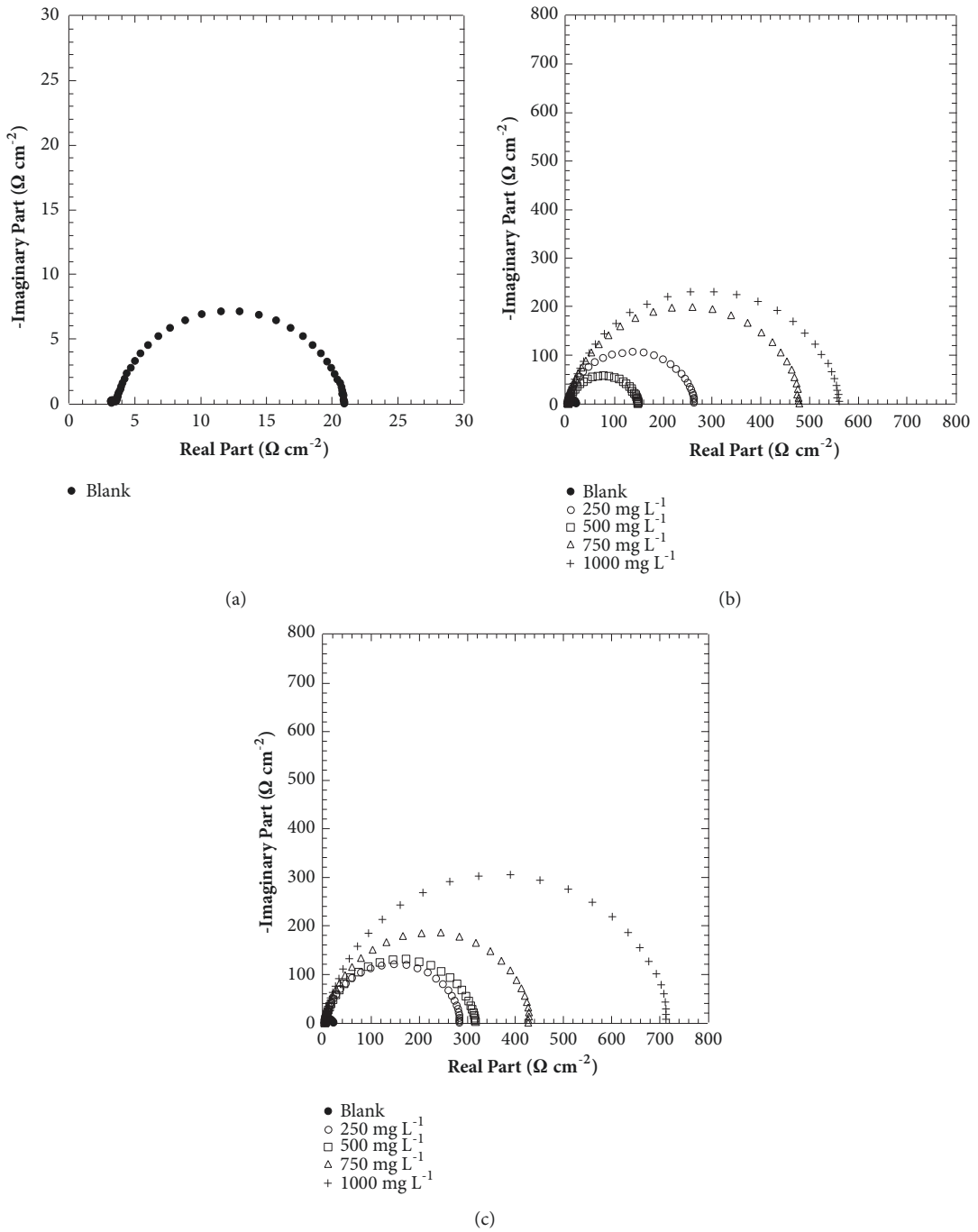

FIGURE 6: Nyquist diagram of carbon steel in 1.0 mol L^{-1} HCl solution without (a) and with inhibitors **1** (b) and **2** (c) at different concentrations.

3.3.2. Electrochemical Impedance Spectroscopy (EIS). The corrosion behavior of carbon steel in 1.0 mol L^{-1} HCl in the absence and presence of triazole compounds (250–1000 mg L^{-1}) was investigated by EIS after immersion for 1 h at room temperature and Figure 6 illustrates the electrochemical impedance diagrams. The impedance data from EIS experiments done in the absence and presence of increasing inhibitors concentrations were summarized in Table 8.

The electrochemical impedance diagrams exhibit one depressed capacitive loop, which indicate a single time constant in the absence and presence of the inhibitors, implying two noteworthy effects: the charge transfer resistance considerably increases and f_{max} decreases when the inhibitors are added. These aforementioned effects decrease the capacitance values, which could be caused by a decrease in the local dielectric constant and/or by a growth in the thickness of the electrical double layer, indicating that the presence of the triazoles compounds changes the electric double-layer structure, which can suggest the inhibitor compounds act by adsorption at the metal/solution interface. The impedance

Table 8: Impedance data obtained from Nyquist diagram of carbon steel in 1.0 mol L^{-1} HCl solution without and with inhibitors at different concentrations.

Inhibitor	Inhibitor Concentration (mg L^{-1})	E_{OCP} (V)	R_{ct} (Ω cm^{-2})	R_s (Ω cm^{-2})	f_{max} (Hz)	C_{dl} (μF cm^{-2})	Efficiency (%)
Blank	0	−0.506	17.344	3.599	199.53	45.99	–
1	250	−0.504	145.12	3.881	39.81	27.55	88
	500	−0.514	261.85	3.928	19.95	30.46	93
	750	−0.505	475.14	4.233	7.94	42.17	96
	1000	−0.500	560.42	3.646	7.94	35.75	97
2	250	−0.505	282.00	3.739	12.59	44.83	94
	500	−0.509	313.41	3.295	12.59	40.34	94
	750	−0.505	426.92	2.762	7.94	46.93	96
	1000	−0.505	714.21	3.677	6.31	35.32	98

diagrams obtained are not perfect semicircle because of the frequency dispersion of the interfacial impedance. This atypical phenomenon is attributed, in the literature, to the nonhomogeneity of the electrode surface rising from the surface roughness or interfacial phenomena [21, 22].

This semicircle intersection with the real axis at high frequencies produces an ohmic resistance (R_s) of nearly 3,6 Ω cm^{-2} of the solution. The solution resistance (R_s) is close in the absence and presence of the inhibitors compounds. The charge transfer resistance (R_{ct}) was calculated from the variance in impedance at lower and higher frequencies. The double-layer capacitance (C_{dl}) was obtained using

$$C_{dl} = \frac{1}{2\pi f_{max} R_{ct}} \quad (10)$$

where f_{max} is the frequency when the imaginary component of the impedance is maximal. A C_{dl} value of 46.0 μF cm^{-2} was found for the carbon steel electrode at 1.0 mol L^{-1} HCl aqueous solution.

From Table 8, it is clear that the R_{ct} values increased with inhibitor concentration increment, which implies a reduction in the active surface area derived by the adsorption of the inhibitors on the carbon steel surface and indicates the corrosion process turned to be hindered. This assumption is supported by the anodic and cathodic polarization curves results. The inhibition efficiency obtained from the R_{ct} values in the absence and presence of inhibitors varied from 88 to 97% in inhibitor **1** and 94 to 98% in inhibitor **2**, over a concentration range of 250–1000 mg L^{-1}.

4. Conclusions

The synthesis of triazoles compound following an easy, low cost, and simplified synthetic route gave good corrosion inhibitors. For this purpose, a range of 250 to 1000 mg L^{-1} was applied in weight loss and electrochemical assays in acid media for ASTM 1020 carbon steel. These assays showed some relevant inhibition efficiency (> 90%) for named inhibitors **1** and **2**. From Langmuir isotherm the adsorption of inhibitors on the carbon steel surface might occur by physical and chemical interaction; however, the activation energy raised suggesting a physisorption process for the interaction of the inhibitor on the carbon steel surface.

For the future, our perspective is the addition of an amount of these inhibitors in commercial anticorrosive inks.

Data Availability

The data used to support the findings of this study are available from the corresponding author upon request.

Conflicts of Interest

The authors declare that they have no conflicts of interest.

Acknowledgments

The authors thank National Council of Technological and Scientific Development (Brazil) for research fellowship support and IFRJ and FAPERJ for the financial support.

References

[1] J. A. Joule and K. Mills, *Heterocyclic Chemistry*, Wiley, 5th edition, 2010.

[2] C. G. de Oliveira, V. W. Faria, G. F. de Andrade et al., "Synthesis of thiourea derivatives and its evaluation as corrosion inhibitor for carbon steel," *Phosphorus, Sulfur, and Silicon and the Related Elements*, vol. 190, no. 8, pp. 1366–1377, 2015.

[3] A. Zarrouk, B. Hammouti, S. S. Al-Deyab et al., "Corrosion inhibition performance of 3,5-Diamino-1,2,4-triazole for Protection of Copper in Nitric Acid Solution," *International Journal of Electrochemistry*, vol. 7, pp. 5997–6011, 2012.

[4] F. M. Al-Kharafi, F. H. Al-Hajjar, and A. Katrib, "3-phenyl-1,2,4-triazol-5-one as a corrosion inhibitor for copper," *Corrosion Science*, vol. 26, pp. 257–264, 1986.

[5] P. G. Fox and P. A. Bradley, "1 : 2 : 4-triazole as a corrosion inhibitor for copper," *Corrosion Science*, vol. 20, pp. 643–649, 1980.

[6] K. R. Ansari, D. K. Yadav, E. E. Ebenso, and M. A. Quraishi, "Corrosion inhibition and adsorption studies of somebarbiturates on mild steel/acid interface," *International Journal of Electrochemical*, vol. 7, pp. 4780–4799, 2012.

[7] M. A. Quraishi, Sudheer, K. R. Ebenso, and E. E. Ebenso, "3-Aryl substituted triazole derivatives as new and effective corrosion inhibitors for mild steel in hydrochloric acid solution," *International Journal of Electrochemcal Science*, vol. 7, pp. 7476–7492, 2012.

[8] H.-L. Wang, H.-B. Fan, and J.-S. Zheng, "Corrosion inhibition of mild steel in hydrochloric acid solution by a mercapto-triazole compound," *Materials Chemistry and Physics*, vol. 77, no. 3, pp. 655–661, 2003.

[9] L. Lin Wang, M. J. Zhu, F. C. Yang, and C. W. Gao, "Study of a triazole derivative as corrosion inhibitor for mild steel in phosphoric acid solution," *International Journal of Corrosion*, vol. 2012, Article ID 573964, 6 pages, 2012.

[10] G. E. Negrón-Silva, R. González-Olvera, D. Angeles-Beltrán et al., "Synthesis of new 1,2,3-triazole derivatives of uracil and thymine with potential inhibitory activity against acidic corrosion of steels," *Molecules*, vol. 18, no. 4, pp. 4613–4627, 2013.

[11] L. M. Alaoui, B. Hammouti, A. Bellaouchou, A. Benbachir, A. Guenbour, and S. Kertit, "Corrosion inhibition and adsorption properties of 3-amino-1,2,3-triazole on mild steel in H_3PO_4," *Der Pharma Chemica*, vol. 3, no. 4, pp. 353–360, 2011.

[12] N. Boechat, V. F. Ferreira, S. B. Ferreira et al., "Novel 1,2,3-triazole derivatives for use against mycobacterium tuberculosis H37Rv (ATCC 27294) strain," *Journal of Medicinal Chemistry*, vol. 54, no. 17, pp. 5988–5999, 2011.

[13] S. Zeghada, G. Bentabed-Ababsa, A. Derdour et al., "A combined experimental and theoretical study of the thermal cycloaddition of aryl azides with activated alkenes," *Organic & Biomolecular Chemistry*, vol. 9, no. 11, pp. 4295–4305, 2011.

[14] S. Ram and R. E. Ehrenkaufer, "Ammonium formate in organic synthesis: a versatile agent in catalytic hydrogen transfer reductions," *Synthesis*, vol. 1988, no. 2, pp. 91–95, 1988.

[15] S. E. Yoo and S. H. Lee, "Reduction of organic compounds with sodium borohydride-copper(II) sulfate system," *Synlett*, no. 7, pp. 419-420, 1990.

[16] S. Jothilakshmi and K. U. Rekha Rekha, "A review of green corrosion inhibitors from plant extracts of various metal in different medium," *Advances in Materials and Corrosion*, vol. 3, pp. 17–19, 2014.

[17] V. Gentil, *Corrosão, 2011, 6^a*, (LTC), Rio de Janeiro, Brazil, 2001.

[18] K. Tebbji, A. Aouniti, A. Attayibat et al., "Inhibition efficiency of two bipyrazole derivatives on steel corrosion in hydrochloric acid media," *Indian Journal of Chemical Technology*, vol. 18, no. 3, pp. 244–253, 2011.

[19] P. P. Kumari, P. Shetty, and S. A. Rao, "Electrochemical measurements for the corrosion inhibition of mild steel in 1 M hydrochloric acid by using an aromatic hydrazide derivative," *Arabian Journal of Chemistry*, vol. 10, pp. 653–663, 2017.

[20] G. M. Pinto, J. Nayak, and A. N. Shetty, "4-(N,N-Diethyl-amino)benzaldehyde thiosemicarbazone as Corrosion Inhibitor for 6061 Al – 15 vol. pct. SiC(p) Composite and its Base alloy," *Materials Chemistry and Physics*, vol. 125, pp. 628–640, 2011.

[21] F. S. De Souza and A. dan Spinelli, "Caffeic acid as a green corrosion inhibitor for mild steel," *Corrosion Science*, vol. 51, no. 3, pp. 642–649, 2009.

[22] A. Ostovari, S. M. Hoseinieh, M. Peikari, S. R. Shadizadeh, and S. J. Hashemi, "Corrosion inhibition of mild steel in 1 M HCl solution by henna extract: a comparative study of the inhibition by henna and its constituents (Lawsone, Gallic acid, α-d-Glucose and Tannic acid)," *Corrosion Science*, vol. 51, no. 9, pp. 1935–1949, 2009.